sciendo

POLISH MARITIME RESEARCH 3 (103) 2019 Vol. 26; pp. 56-64
10.2478/pomr-2019-0046

NUMERICAL INVESTIGATING THE EFFECT OF WATER DEPTH ON SHIP RESISTANCE USING RANS CFD METHOD

Nguyen Thi Ngoc Hoa [a]
Vu Ngoc Bich [a]
Tran Ngoc Tu [b]
Nguyen Manh Chien [b]
Le Tat Hien [c]
[a] Ho Chi Minh City University of Transport, Vietnam
[b] Vietnam Maritime University, Vietnam
[c] Hochiminh City University of Technology, Vietnam National University, Vietnam

ABSTRACT

On inland waterways the ship resistance and propulsive characteristics are strictly related to the depth of the waterway, thus it is important to have an understanding of the influence of water depth on ship hydrodynamic characteristics. Therefore, accurate predictions of hydrodynamic forces in restricted waterways are required and important. The aim of this paper is investigating the capability of the commercial unsteady Reynolds– Averaged Navier–Stokes (RANS) solver to predict the influence of water depth on ship resistance. The volume of fluid method (VOF) is applied to simulate the free surface flow around the ship. The hull resistance in shallow and deep water is compared. The obtained numerical results are validated against related experimental studies available in the literature.

Keywords: ship resistance, shallow water, RANS

INTRODUCTION

In general, for a ship moving in shallow water, the following phenomena may take place due to the interaction between the ship and the seabed [1, 2]:

- water speed around the ship hull increases;
- pressure gradients around the hull increase;
- dynamic trim and sinkage increase;
- ship's wave pattern changes (wave amplitude increases);
- ship resistance increases;
- other ship characteristics (wake field, hull-propeller interaction, maneuverability) change;

The knowledge of ship resistance when navigating through shallow water regions is necessary and important, as correct design of ship propulsion system depends on the accuracy in determining its resistance.

This paper discusses the influence of water depth on ship resistance, with the aim to make inland vessels operate more economically and safely, as well as to reduce their fuel consumption.

There are three types of methods which are used to evaluate ship resistance in shallow water: empirical methods, Computational Fluid Dynamics (CFD) methods, and model towing tank tests.

The model tests give the most reliable results in predicting ship resistance in comparison with the two other methods. But this technique is both expensive and time consuming, so it is usually used after the alternative design stage, when the overall dimensions and the lines plan of the ship have already been optimally chosen.

Some empirical methods, mostly based on towing tank test results, have been proposed by Artjushkov [3], Geerts [4], and Karpov [5], among others, to predict ship resistance in shallow water. These methods are fast and do not require much input data. However, their range of application is often limited, and the lack of accuracy is a problem [6].

Nowadays, fast development of computational resources is making the Computation Fluid Dynamics (CFD) methods become a powerful tool for ship designers in solving problems related to hydrodynamics. Ship resistance calculation is one of

the basic hydrodynamic problems. The benefit of this method is that it allows visualization of several quantities, such as flow streamlines, wave profiles, or pressure distributions, for instance, which are difficult to obtain from experiments. This is a very useful aid for designers to understand the physics of flow phenomena, at least from a qualitative point of view.

Depending on the assumptions made to simplify the fluid equations, a number of CFD approaches can be named that are available to solve hydrodynamics problems. These approaches include: the potential flow theory (panel code), Reynold Averaged Navier-Stokes (RANS) equations, Detached Eddy Simulation (DES), and Large Eddy Simulation (LES). DES and LES approaches require much more computational effort, in terms of meshing and solver time, than the remaining two methods, but they allow to capture small variances of quantities of interest (velocity and pressure). However, in the ship resistance problem we mainly focus on the average values of forces. The RANS method simulates the turbulence using the term called "turbulence model" and gives time averaged mean values for velocity and pressure fields. This way, it consumes less time and requires less computational resources [7].

At the moment, the most popular approach is RANS CFD, as it ensures sufficient accuracy of results for engineering purposes at reasonable computational time. However, the level of accuracy of the numerical simulation significantly depends on practical skills.

There are some authors who performed shallow-water CFD calculations to investigate the influence of shallow water on ship resistance. However, large discrepancies between CFD and experimental data were witnessed for some results obtained by Prakash et al. [8], Pacuraru et al. [9], Patel et al. [10], Tezdogan et al. [11].

This paper presents the theoretical background and application of the RANS method to investigate the effect of water depth on ship resistance, taking into account the detailed setup of simulation to get accurate and meaningful results which agree well with the experiment. The case study is the US Navy Combatant DTMB with the available experimental data making it possible to validate the obtained numerical results on the experiment. The commercial solver Star–CCM+ was used in this study. The main objective of the paper is to assess the accuracy of CFD simulation for ship resistance calculations at different water depths.

The paper is organized as follows: the theoretical background of shallow water effects on ship wave patterns and ship resistance are described in detail in Section 2. The numerical simulation is analyzed and discussed in Section 3. The summary and conclusions are presented in Section 4.

THEORETICAL BACKGROUND OF RESTRICTED WATER EFFECTS ON WAVE PATTERNS AND SHIP RESISTANCE

When the ship approaches a restricted depth water region, the interaction begins between the ship and the seabed, which leads to the velocity increase and pressure decrease under the hull, and significant changes in sinkage and trim. All this leads to the increase in potential and skin friction drag, together with the increase in wave resistance. Using the wave theory, the wave velocity c can be developed in terms of h and λ, where h is the water depth from the still water level and λ is the wavelength, crest to crest. Therefore, classifying the water as deep or shallow can be decided based on the ratio of water depth h to wavelength λ.

For the deep water, the ratio h/λ is approximately assumed as $h/\lambda \geq 1/2$.

For the shallow water, the ratio h/λ is $h/\lambda \leq 1/2$ and $c = \sqrt{gh}$ is known as the critical speed, where c is the wave velocity and g is the acceleration gravity.

Larsson et al. [1] performed shallow water investigations in which they presented wave patterns formed due to a point source in shallow water. Their work led to the introduction of the dimensionless depth Froude number:

$$Fr_h = \frac{V}{\sqrt{gh}} \tag{1}$$

SHALLOW WATER EFFECTS ON SHIP WAVE PATTERNS

Obviously, the geometry of the ship's wave pattern in shallow water is not only dependent on its Froude number but also on its depth Froude number, which modifies the wave length and wave components. Based on the value of Fr_h, there are three flow regimes:

- Sub-critical $Fr_h < 1.0$;
- Critical $Fr_h = 1.0$;
- Supercritical $Fr_h > 1.0$.

The wave system at speeds well below $Fr_h < 1.0$, is shown in Figure 1(a). It comprises the transverse wave system and the divergent wave system propagating away from the ship. This wave system might be called the Kelvin wave pattern. When the ship speed nears the critical speed, $Fr_h = 1.0$ the waves become more perpendicular to the track of the ship, Figure 1(b). At speeds greater than the critical speed, the diverging wave system propagates away from the ship with a certain angle, but in this case the transverse waves are clearly visible [1].

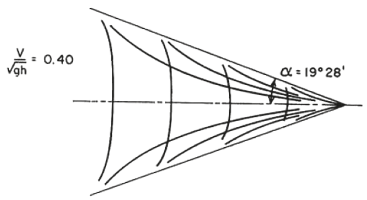

a) Sub-critical

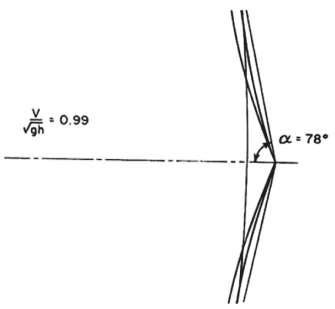

b) Critical

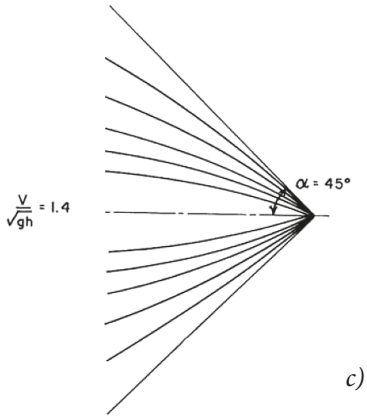

Fig. 1. Pressure patch wave patterns for different Fr_h [1]

SHALLOW WATER EFFECTS ON SHIP RESISTANCE

In order to describe fully the effect of shallow water on ship resistance, it is usual to use such parameters as T/h or L/h, as well as the depth Froude number Fr_h. The influence of shallow water on the wave resistance component caused by changes in the wave pattern has already been investigated by Larsson et al. [1]. The results of the Froude number-based resistance experiment regarding to L/h changes are shown in Figure 2.

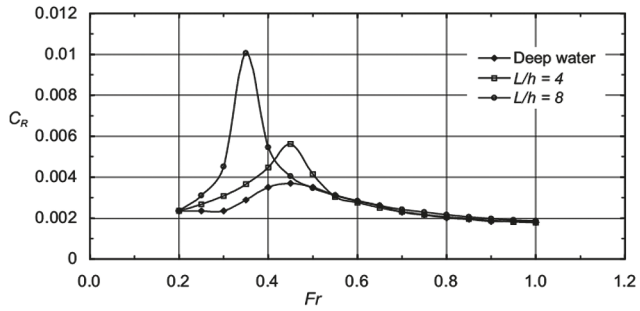

Fig. 2. Influence of water depth on residual resistance coefficient [12]

Figure 3 shows the influence of water depth on the total resistance coefficient as a function of Froude number and depth Froude numbers.

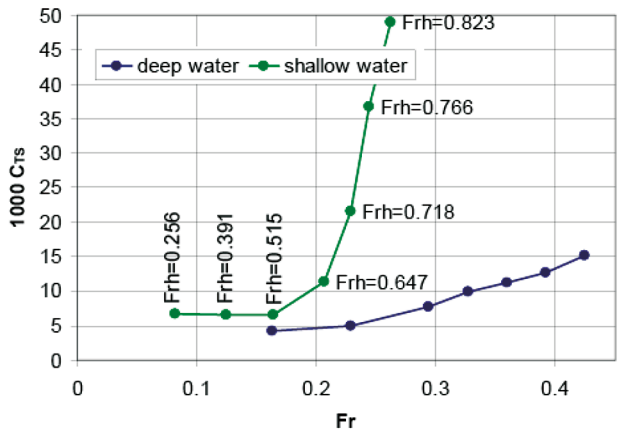

Fig. 3. Influence of water depth on total resistance coefficient

NUMERICAL SIMULATIONS

REFERENCE VESSEL

The vessel under study in this paper is the US Navy Combatant DTMB shown in Figure 4. The main reason for selecting this hull is that the hull geometry is published [13] and extensive model test data exists for vessel resistance at different Froude numbers in shallow and deep water. This data comes from tests carried out by the Ship Design and Research Centre CTO S.A. Poland [14, 15]. To provide opportunities for direct comparison, the computations were performed at the model scale with scale factor $\lambda = 26.69$, the same as the scale used in model tests.

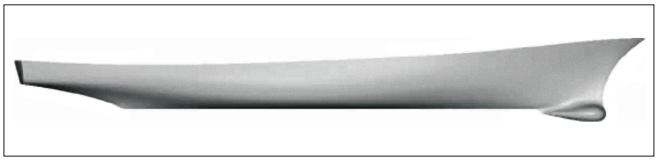

Fig. 4. Geometry of US Navy Combatant DTMB

Tab. 1. Basic parameters of unmanned boats

Description		Ship	Model
Scale factor	λ	–	26.69
Length between perpendiculars	L_{PP}(m)	142.0	5.320
Length of waterline	L_{WL}(m)	142.18	5.327
Breadth	B(m)	19.06	0.714
Draft	T(m)	6.15	0.230
Volume	∇(m^3)	8425	0.438
Wetted surface	S(m^2)	2972	4.17
Longitudinal Center of Buoyancy From AP	LCB/ L_{PP}	0.489	

TEST CASES

The computations were performed on the model scale for the following conditions: design draft $T_M = 0.23$ m corresponding to the model volume $\nabla_M = 0.455$ m^3, and LCB measured from AP equal to 2.602 m in shallow water (water depth $h_M = 0.46$ m) and in deep water.

The following settings were considered in the simulations:

- Calm water condition;
- Six model scale speeds: 0.597; 0.799, 0.995; 1.199; 1.291, 1.394 m/s for shallow water and deep-water simulations, corresponding to six depth Froude numbers: 0.281, 0.376, 0.469, 0.564, 0.608, 0.656 for shallow water case.
- The vessel is free to trim and sink;
- The hull mass is constant.

The water parameters for all case studies (density, viscosity) corresponded to real values used in the experimental set up (water density $\rho = 998.7$ kg/m^3, kinematic viscosity of water $\nu = 1.079 \times 10^{-6}$ m^2/s).

COMPUTATION SETUP

The commercial package Star-CCM+ from Siemens was used for the computation.

Computational domain and boundary conditions

The size of computational domain and the boundary conditions are important factors that affect the numerical results. For the computational domain, in general, its size should be taken sufficiently large to avoid any wave reflections from the boundary walls that might affect the numerical results. For the ship resistance calculation, the existing flow symmetry makes that only half of the hull (port side) can be simulated, thus reducing the computational time. Based on the recommendations and applications reported in Star-CCM+ [16], the size of the computational domain used in this study was selected as follows: the inlet boundary was located at $1.5L_{pp}$ from forward perpendicular, while the outlet boundary was located at $2.5L_{pp}$ from aft perpendicular. The top boundary was located at $1.5L_{pp}$ from the free surface, and the lateral boundary at $2.5L_{pp}$ from the center plane. The bottom boundaries for shallow-water and deep-water simulations were located at depth of 0.46 m and $2.5L_{pp}$ from the free surface, respectively. The free surface was located at z = 0.

There are several types of boundary conditions offered by the CFD software package. For Star-CCM+, the boundary conditions applied when simulating ship resistance in shallow and deep water are given in Table 2.

Tab. 2. Boundary Conditions

Boundary	Shallow water	Deep water
Inlet	Velocity inlet	Velocity inlet
outlet	Pressure outlet	Pressure outlet
side	Symmetry plane	Symmetry plane
Symmetry	Symmetry plane	Symmetry plane
Top	Velocity inlet	Velocity inlet
Bottom	Moving No-slip wall	Velocity inlet
Ship hull	No-slip wall	No-slip wall

In the case of shallow water simulation, there is an interaction between the ship and the seabed. Therefore, the moving No-slip wall condition was applied on the tank bottom (the bottom moves with the velocity equal to the ship speed), which is similar to the CFD simulation successfully performed by Mark Bettle et. al [17].

Physics modelling

The computation was carried out using the unsteady Reynold Averaged Navier-Stokes (RANS) equation model. The free surface was modeled with the volume of fluid (VOF) method. Fluid turbulence was simulated employing the Realizable K-epsilon Two-layer model with Two-layer all y+ wall treatment. To ensure accurate representation of ship motions, Star-CCM+ offers a Dynamic Fluid-Body Interaction (DFBI) module, which allows the user to select degrees of freedom in which the analyzed structure can move and rotate. For the current study, the ship was free to trim and sink.

Since the ship moves in shallow water, the bottom of the ship is very close to the seabed boundary. To accurately model the movement of the ship above the fixed bottom, the "morphing mesh" was used. When using this mesh, the boundaries of a region can change position and shape over time, due to the motion of the contacting body [16]. Figure 5 shows a simple example of the morphing mesh with the flow through a cylinder with contracting wall.

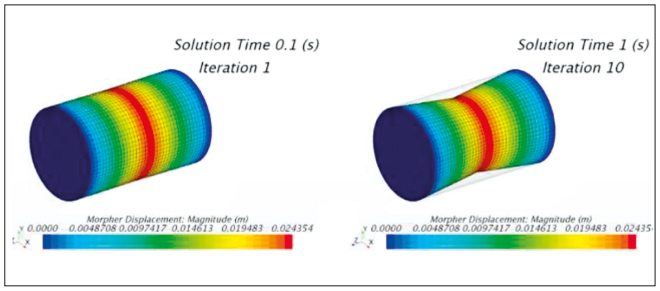

Fig. 5. Example of morphing mesh [16]

Mesh generation

The mesh used in the calculations was composed of hexahedral cells. The meshing and the flow simulation were conducted by Star-CCM+. The grid generated for DTMB was characterized by concentration of cells around the hull region near the free surface.

To avoid using a fine mesh where unnecessary, a local volume was created for the sonar dome, and particular cell size was assigned. To capture the exact flow behavior near the walls of the wetted surface, prism layers were used to resolve the near-wall flow accurately. The prism layer numbers were selected such as to ensure the average y+ value of 50 on ship wall boundaries. To capture the flow around the hull near the free surface, a finer mesh was created in the free surface region. The grid at the free surface needed to be small enough to capture the wave elevation.

Figure 6 shows the general view of the coarsest mesh for shallow and deep water.

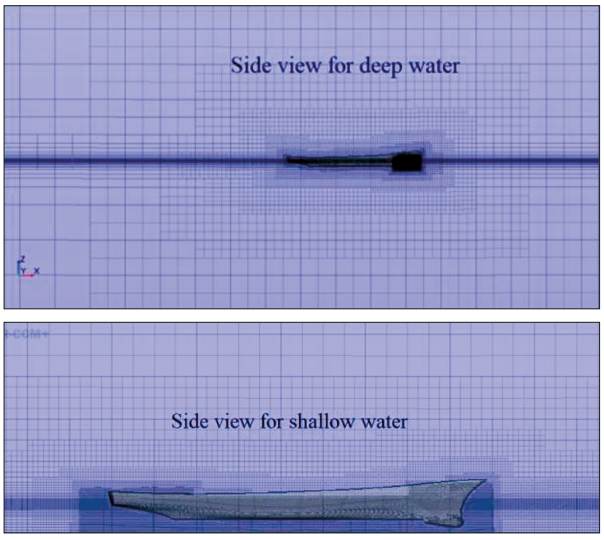

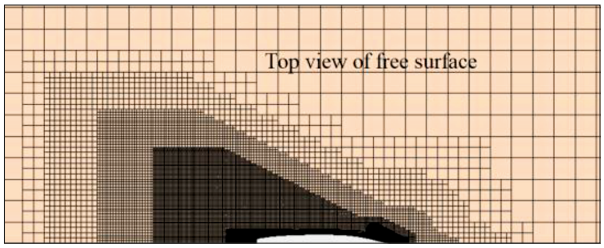

Fig. 6. General view of computational mesh in shallow and deep water

Selection of time step

One of the key issues determining the numerical accuracy is the time step. For implicit solvers, the time step is decided by flow features. For standard pseudo-transient resistance computations, the recommended time step is related to the L/V ratio [18]:

$$\Delta t = 0.005 \sim 0.01\ L/V,\ [\mathrm{s}] \tag{2}$$

where V [m/s] is the ship speed and L [m] is the characteristic length.

RESULTS AND DISCUSSION

Mesh independency study

The first step of the research was to carry out the mesh sensitivity study, i.e. to determine the mesh density at which the difference between total resistance values obtained from two subsequent meshes reaches a sufficiently low level. The goal of such a study is to obtain the "grid-independent solution", i.e. to ensure that further mesh refinement does not improve the quality of the results. In the presented case, the mesh sensitivity was studied for shallow water and deep-water cases at V = 1.199 m/s. The studies were conducted using three grids with the Non-integer grid refinement ratio $r_G = \sqrt{2}$ (the value recommended by the ITTC-Quality Manual 7.5-03-01-01, 2008 [19]). These grids were referred to as coarse (grid#3), medium (grid#2) and fine grid (grid#1), with the corresponding cell numbers equal to 0.54, 1.23 and 2.85 million, respectively, for shallow water, and 0.65, 1.42 and 2.97 million for deep water. Mesh refinement was done by reducing the cell size in all directions outside the prism layer. The idea here was to keep the same y+ values, of about 40 to 60, at near-wall cells over the largest part of the wetted hull surface for all six cases.

Table 3 presents the total resistance results obtained for three grids resolutions at V = 1.199 m/s in shallow and deep water. The difference between the EXP data, denoted as D, and the CFD simulation results, denoted S in this paper, is defined as:

$$E\%\,D = \frac{(D-S)}{D}.100\% \tag{3}$$

The solution changes obtained in simulations performed on two subsequent meshes, such as fine-medium ε_{12} and medium-coarse ε_{23}, are defined as follows:

$$\varepsilon_{12}\% = (S_1 - S_2) / S_1;\ \ \varepsilon_{23}\% = (S_2 - S_3) / S_2 \tag{4}$$

The presented cases show that the resistance changes monotonically with mesh density, and the comparison shows quite a good agreement between simulation (CFD) and experimental values (EFD), especially for the fine mesh (the relative error equal to only 3.28% for shallow water simulation and 0.47% for deep water simulation). As a result, the fine mesh was used in further studies.

Numerical simulation results

Table 4 and Figure 7 compare the predicted and measured total ship resistance values in shallow and deep water for the depth Froude number ranging from 0.281 to 0.656. As can be seen, the difference between the numerically predicted and experimentally recorded ship resistance results varies from 1.45% to 4.47% for the shallow-water simulation and from 0.47% to 3.57% for the deep-water simulation.

Comparing the values of ship resistance components for shallow and deep water is summarized in Table 5 and Figure 8. As can be seen, two of the resistance components increase when the ship moves in shallow water. The change of the friction resistance component can be explained by the

Tab. 3. Total resistance predicted on different grids at V = 1.199 m/s (Fr_h = 0.564) in shallow and deep water (Model scale)

Shallow water							
Parameter		EFD(D)	V&V Study			ε_{32}%	ε_{12}%
			Grid#3	Grid#2	Grid#1		
RT[N]	Value	15.291	14.23	14.68	14.79	3.07	0.74
	E%D	/	6.94	4.00	3.28		
Deep water							
Parameter		EFD(D)	V&V Study			ε_{32}%	ε_{12}%
			Grid#3	Grid#2	Grid#1		
RT[N]	Value	12.720	12.98	12.84	12.78	–1.09	–0.47
	E%D	/	–2.04	–0.94	–0.47		

Tab. 4. Comparing predicted ship resistance results with experimental values (model scale)

Parameters	V [m/s]	0.597	0.799	0.995	1.199	1.291	1.393
R_T [N] in shallow water (h = 0.46m)	Fr_h	0.281	0.376	0.469	0.564	0.608	0.656
	EXP.	4.670	7.282	10.667	15.291	16.695	19.788
	CFD	4.47	7.05	10.28	14.79	16.953	20.08
	Relative error [%]	4.47	3.28	3.77	3.39	–1.52	–1.45
R_T [N] in deep water	EXP.	3.08	5.27	8.25	12.72	14.52	16.98
	CFD	3.19	5.45	8.48	12.78	14.78	17.43
	Relative error [%]	3.57	3.42	2.79	0.47	1.79	2.65

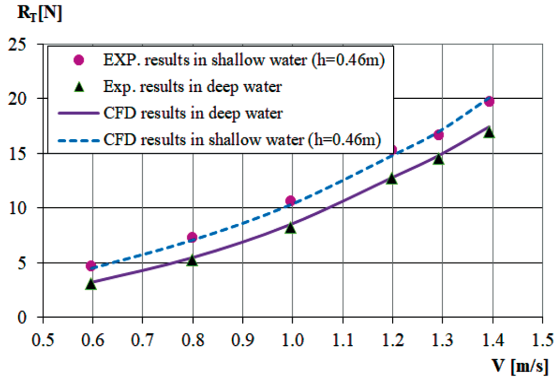

Fig. 7. Comparing predicted ship resistance results in deep and shallow water at different speeds with experimental values

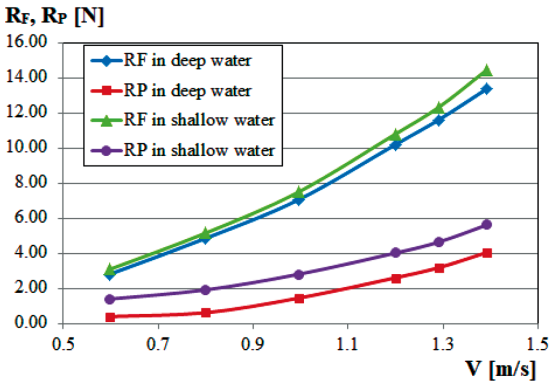

Fig. 8. Changes of ship resistance components in shallow and deep water

Tab. 5. Changes of ship resistance components in shallow and deep water (model scale)

V [m/s]	CFD computation in deep water			CFD computation in shallow water (h = 0.46m)			
	R_T	R_F	R_P	Fr_h	R_T	R_F	R_P
0.597	3.19	2.80	0.39	0.281	4.47	3.08	1.39
0.799	5.45	4.84	0.61	0.376	7.05	5.14	1.91
0.995	8.48	7.04	1.44	0.469	10.28	7.48	2.80
1.199	12.78	10.18	2.6	0.564	14.79	10.78	4.01
1.291	14.78	11.6	3.18	0.608	16.953	12.316	4.64
1.393	17.43	13.38	4.05	0.656	20.08	14.46	5.62

increasing flow velocity under the keel when the vessel moves from deep to shallow water. This flow velocity change, clearly shown in Figure 9, results from the interaction between the ship and the seabed. The change of the pressure resistance component can be explained by the change of the wave pattern in shallow water, accompanied by significant pressure drop (see Figures 10 and 11).

CONCLUSION

The unsteady RANS calculations were performed to predict the resistance of the DTMB model in shallow water at different depth Froude numbers. The selected ship speed values were the same as in the towing tank experiments performed in CTO [14, 15]. In all analyses, use was made of the commercial RANS solver Star-CCM+ version 12.02.011.R8.

The predicted ship resistance and model test results were presented for the DTMB model. The CFD results obtained for all simulation cases show quite good agreement with the experiment.

The increase of ship resistance in shallow water, compared to the deep-water case at the same speed, is due flow velocity change under the keel and significant pressure drop along the hull, all this leading to wave pattern change.

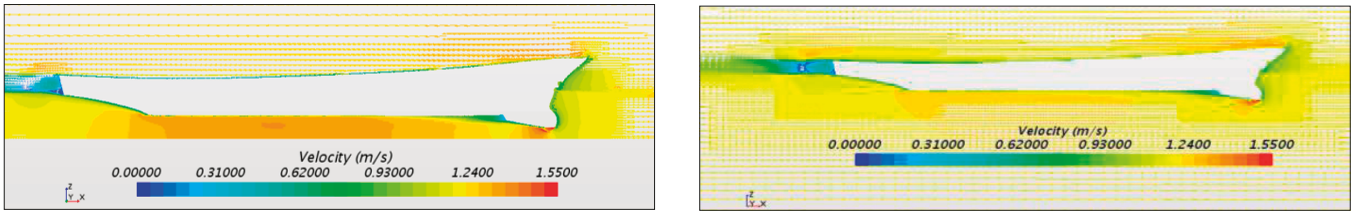

a) Shallow water b) Deep water

Fig. 9. Flow velocity distributions under keel in deep and shallow water, at the same speed (V=1.199 m/s)

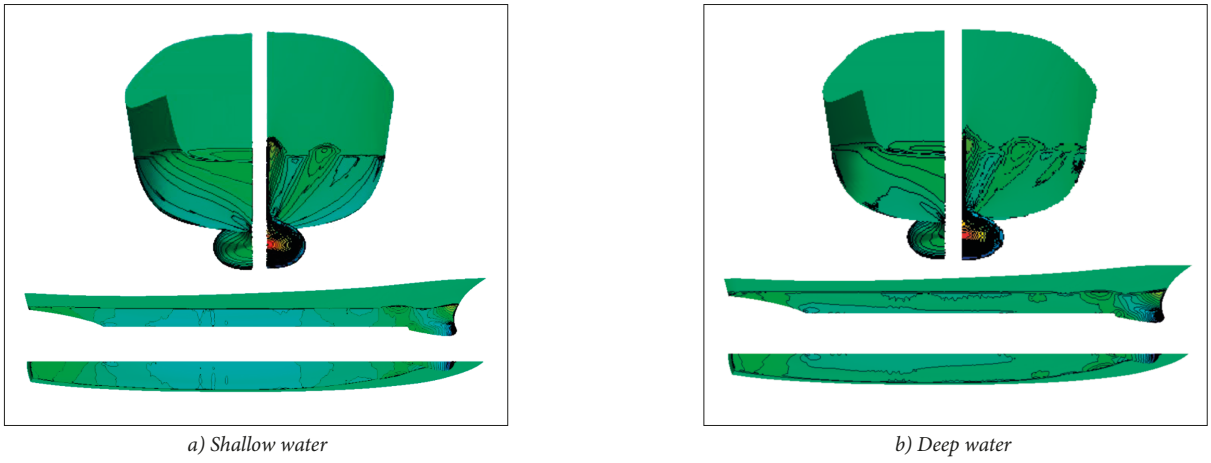

a) Shallow water b) Deep water

Fig. 10. Dynamic pressure distributions along the hull in deep and shallow water,at the same speed (V=1.199 m/s)

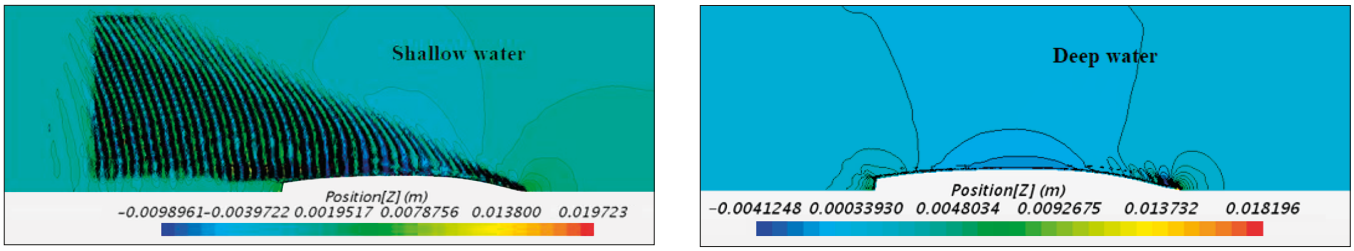

a) wave patterns at V=0.799 m/s

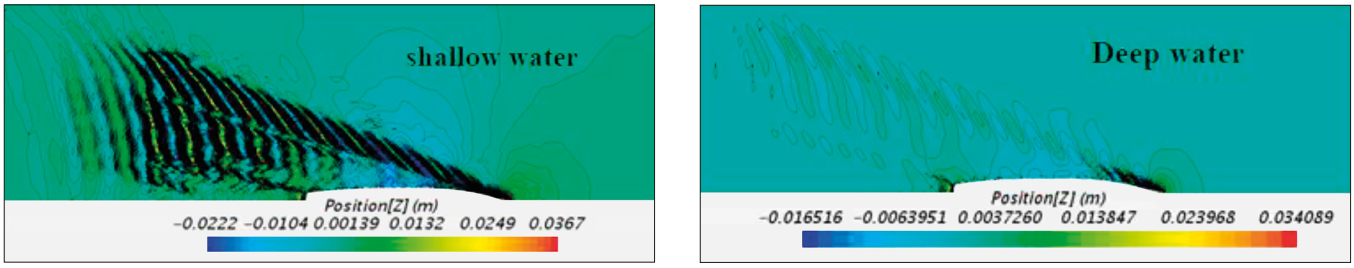

b) wave patterns at V=1.199 m/s

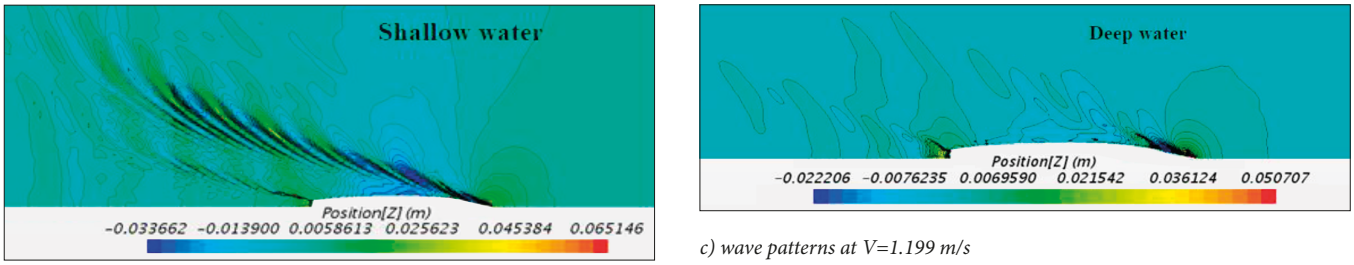

c) wave patterns at V=1.199 m/s

Fig. 11. Wave patterns at different speeds in shallow and deep water

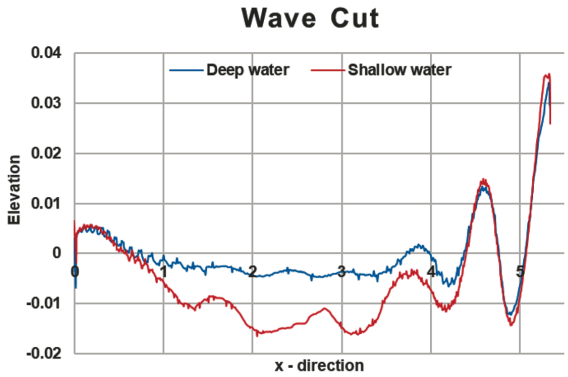

Fig. 12. Wave cut at V = 1.199 m/s in shallow and deep water

The computed values of the resistance components (frictional and pressure) reveal that when the ship moves in shallow water, the pressure resistance component changes more than the friction resistance component, especially at high depth Froude numbers.

Good agreement between CFD computations and model tests illustrates the capability of RANS CFD in solving ship hydrodynamics problems. However, further validation using model tests with final hull form should be carried out to avoid unexpected errors of numerical methods.

NOMENCLATURE

B [m] – *Ship breadth*
L_{PP} [m] – *Length between perpendiculars*
L_{WL} [m] – *Length at water level*
∇[m^3] – *Ship volume displacement*
S [m^2] – *Wetted surface area*
T [m] – *Ship draft*
R_T [N] – *Total ship resistance*
R_F [N] – *Friction resistance component*
R_p [N] – *Pressure resistance component*
h [m] – *Depth of water*
V [m/s] – *Ship speed*
Fr_h – *Depth Froude number*
p [kg/m^3] – *Water density*

REFERENCES

1. Larsson, L. and H. Raven, *Ship resistance and flow*. 2010: Society of Naval Architects and Marine Engineers.

2. Bertram, V., *Practical ship hydrodynamics*. 2011: Elsevier.

3. Artjushkov, L., *Wall effect correction for shallow water model tests*. NE Coast Institution of Engineers and Shipbuilders., 1968.

4. Geerts, S., Verwerft, B., Vantorre, M., and Van Rompuy, F., *Improving the efficiency of small inland vessels*. Proc., 7th European Inland Waterway Navigation Conf., Budapest Univ. of Technology and Economics, Budapest, Hungary., 2010.

5. Karpov, A., *Calculation of ship resistance in restricted waters*. TRUDY GII. T. IV, Vol. 2 (in Russian). 1946.

6. Linde, F., et al., *Three-Dimensional Numerical Simulation of Ship Resistance in Restricted Waterways: Effect of Ship Sinkage and Channel Restriction*. Journal of Waterway, Port, Coastal, and Ocean Engineering, 2016. 143(1): p. 06016003.

7. *ITTC 2014 Specialist committee on CFD in marine hydrodynamics—27th* ITTC.

8. Prakash, S. and B. Chandra, *Numerical estimation of shallow water resistance of a river-sea ship using CFD*. International journal of computer applications, 2013. 71(5).

9. Pacuraru, F. and L. Domnisoru. *Numerical investigation of shallow water effect on a barge ship resistance. in IOP Conference Series: Materials Science and Engineering*. 2017. IOP Publishing.

10. Patel, P.K. and M. Premchand, *Numerical investigation of the influence of water depth on ship resistance*. International Journal of Computer Applications, 2015. 116(17).

11. Tezdogan, T., A. Incecik, and O. Turan, *A numerical investigation of the squat and resistance of ships advancing through a canal using CFD*. Journal of Marine Science and Technology, 2016. 21(1): p. 86–101.

12. Molland, A.F., S.R. Turnock, and D.A. Hudson, *Ship resistance and propulsion*. 2017: Cambridge university press.

13. http://www.simman2008.dk/5415/combatant.html.

14. *Resistance test report in deep water for DTMB vessel*. CTO, Poland 2017.

15. *Resistance test report in shallow water for DTMB vessel*. CTO, Poland 2017.

16. *CD-ADAPCO. User Guide STAR-CCM+, Version 13.02*. 2018.

17. Bettle, M., S.L. Toxopeus, and A. Gerber, *Calculation of bottom clearance effects on Walrus submarine hydrodynamics*. International Shipbuilding Progress, 2010. 57(3-4): p. 101–125.

18. *ITTC 2011b Recommended procedures and guidelines 7.5-03-02-03*.

19. *ITTC-Quality Manual 7.5-03-01-01, 2008*.

CONTACT WITH THE AUTHORS

Nguyen Thi Ngoc Hoa
e-mail: hoa_vt@hcmutrans.edu.vn

Vu Ngoc Bich
e-mail: vubich@hcmutrans.edu.vn

Ho Chi Minh City University of Transport
Vietnam